

# PREDICTION OF MECHANICAL PROPERTIES OF HYBRID DISCONTINUOUS COMPOSITES

Joël Henry<sup>1</sup>, Soraia Pimenta<sup>1</sup>, HaNa Yu<sup>2</sup>, Marco Longana<sup>2</sup>

<sup>1</sup>meComposites, Mechanical Engineering Department, Imperial College London, South Kensington  
Campus, London, SW7 2AZ, UK

Email: joel.henry13@imperial.ac.uk, soraia.pimenta@imperial.ac.uk

<sup>2</sup>Advanced Composites Centre for Innovation and Science, University of Bristol, Queen's Building,  
University Walk, Bristol BS8 1TR, UK

**Keywords:** Brick-and-mortar architecture, Hybrid composites, Analytical modelling, Bioinspired composites, Mechanical properties

## Abstract

Composites are widely used for their high mechanical properties and light weight, but remain brittle and expensive. To tackle these issues, a model has been developed to study composite materials combining (i) the brick-and-mortar architecture found in natural composites to increase the toughness, and (ii) hybridisation to tailor further the mechanical response and reduce the material cost. The model can derive the mechanical properties of various discontinuous hybrid architectures and showed remarkably good agreement with both FE and experimental results. Its fully analytical aspect makes it suitable for parametric studies and it can be used as a tool to find optimum configurations and tailor the material for specific applications.

## 1. Introduction

High performance composites combine various advantages compared to more classical metallic materials such as lightweight, high stiffness and high strength. However, their inherent low damage tolerance as well as their high production cost have slowed down their spread to a wider range of industries and applications [1, 2].

A widely known approach to design a damage tolerant structure is to use a discontinuous architecture [3]. This approach, inspired from natural composites (nacre, bone, spider silk), allows to change the failure mode of the composite from brittle fracture of the inclusions to a more progressive failure of the matrix, thus increasing the ductility and energy absorption of the material [3, 4].

An other alternative to overcome the brittleness of composites is hybridisation [5]. Hybrid composites, made of at least two different types of fibres, offer the possibility to tailor the material properties to specific applications, and allow a potential reduction of material costs, for example with the addition of cheaper glass fibres in more expensive carbon-fibre composites [5].

This work aims at bridging the two strategies mentioned above by developing two analytical models to predict the mechanical behaviour of discontinuous hybrid composites. The models are developed in Section 2, and Section 3 presents and discusses the main results. Finally, Section 4 draws the main conclusions.

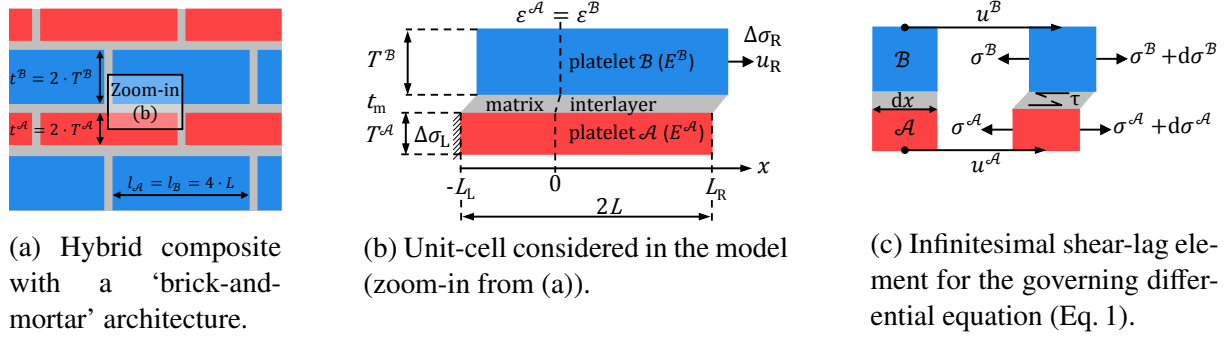


**Figure 1.** Overview of the shear-lag model for brick-and-mortar hybrid composites.

## 2. Model development

### 2.1. Hybrid "brick-and-mortar" architecture

The first model considers the architecture presented in Fig. 1, consisting of a "brick-and-mortar" arrangement with two types of platelets  $\mathcal{A}$  and  $\mathcal{B}$ . The platelets are considered as linear-elastic and are characterised by their Young Moduli  $E^{\mathcal{A}}$  and  $E^{\mathcal{B}}$  and their characteristic thicknesses ( $T^{\mathcal{A}}$  and  $T^{\mathcal{B}}$ , which are half the thickness of each platelet). The matrix interlayer (thickness  $t_m$ ) is characterised by a piecewise linear but otherwise generic constitutive law in shear, where each linear piece  $[i]$  is defined by a tangent stiffness  $G^{[i]}$  (which can be positive or negative). From a shear lag model applied to Fig. 1c, the compatibility of displacements and the equilibrium of stresses can be combined in the following equation:

$$\frac{d^2 \Delta \sigma(x)}{dx^2} = \text{sign}(G) \cdot \lambda^2 \cdot (\Delta \sigma(x) - K \cdot \sigma^\infty), \quad \text{where} \quad \begin{cases} K = \frac{2 \cdot \Delta E \cdot \Sigma T}{\Sigma E \cdot \Sigma T + \Delta E \cdot \Delta T} \\ \lambda = \sqrt{\frac{8 \cdot |G| \cdot (\Sigma E \cdot \Sigma T + \Delta E \cdot \Delta T)}{t_m \cdot (\Sigma E^2 - \Delta E^2) \cdot (\Sigma T^2 - \Delta T^2)}} \end{cases}, \quad (1)$$

and where we define the difference  $\Delta \chi = \chi^{\mathcal{B}} - \chi^{\mathcal{A}}$  and sum  $\Sigma \chi = \chi^{\mathcal{B}} + \chi^{\mathcal{A}}$  for any variable  $\chi$ . Solving Eq. 1 for different values of  $G^{[i]}$  and applying the relevant boundary conditions to the unit cell (Fig. 1b), the stresses in the platelets can be derived, and the full stress-strain curve of the material can be calculated in less than a second (see Section 3.1 for results).

### 2.2. Aligned intermingled architecture

The model described in the previous section can also be used to derive the mechanical response of more complex (and hence realistic) aligned intermingled hybrids composites (Fig. 2a), accounting for a random distribution of fibre types and location of fibre-ends. Because the previous model considered platelets, while the intermingled architecture consists of fibres with circular cross-section (with diameters  $\phi_f^{\mathcal{A}}$  and  $\phi_f^{\mathcal{B}}$ ), the characteristic thicknesses of the fibres can be calculated as  $T = \phi_f/4$ . Moreover, the equivalent matrix thickness  $t_m$  is derived so that both fibre types are associated to a layer of matrix of consistent thickness ( $t_m$  in Fig. 2e), and the overall fibre volume fraction  $V_f$  is defined as an input.

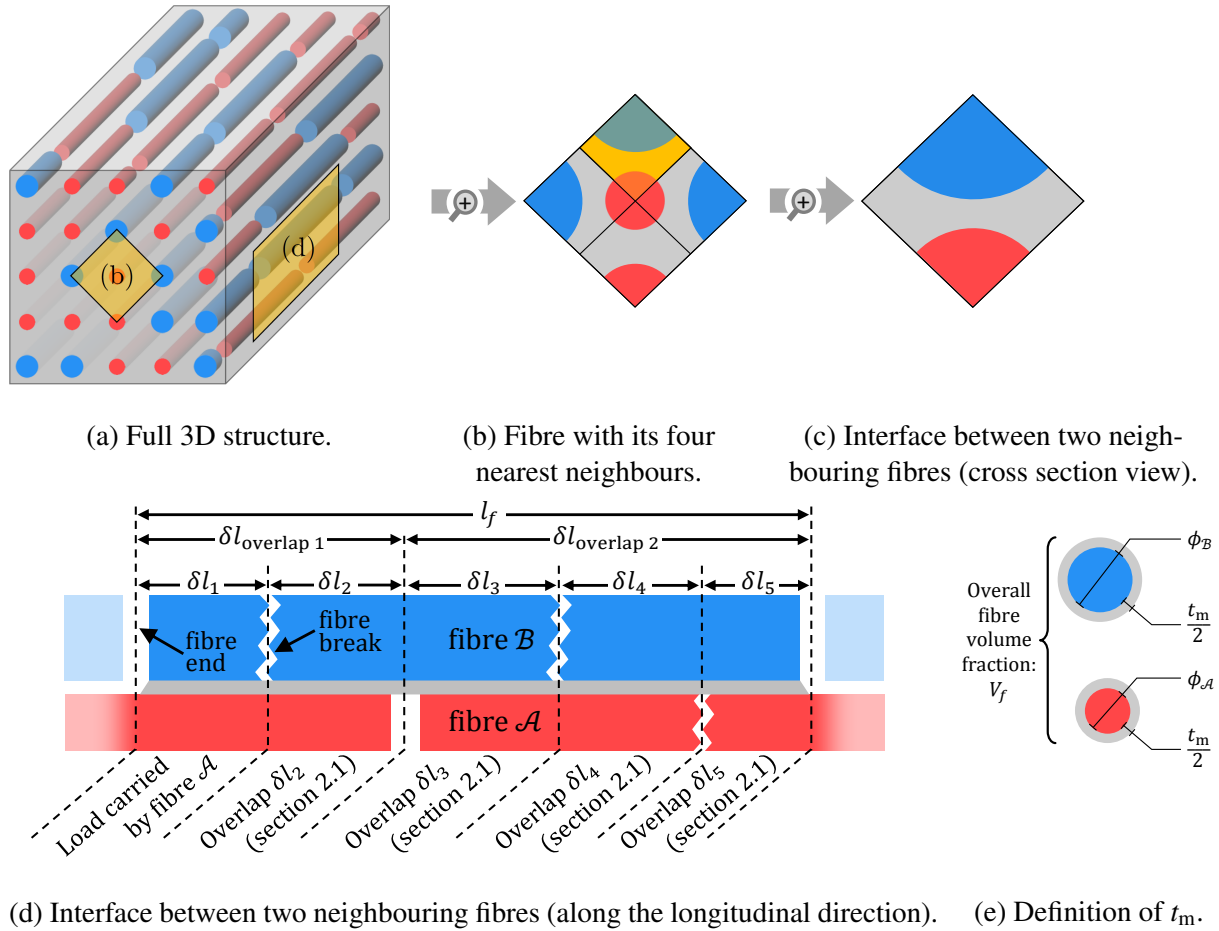


**Figure 2.** Overview of the different scales involved in the model for aligned intermingled hybrid composites.

The model for intermingled hybrid composites runs as follow:

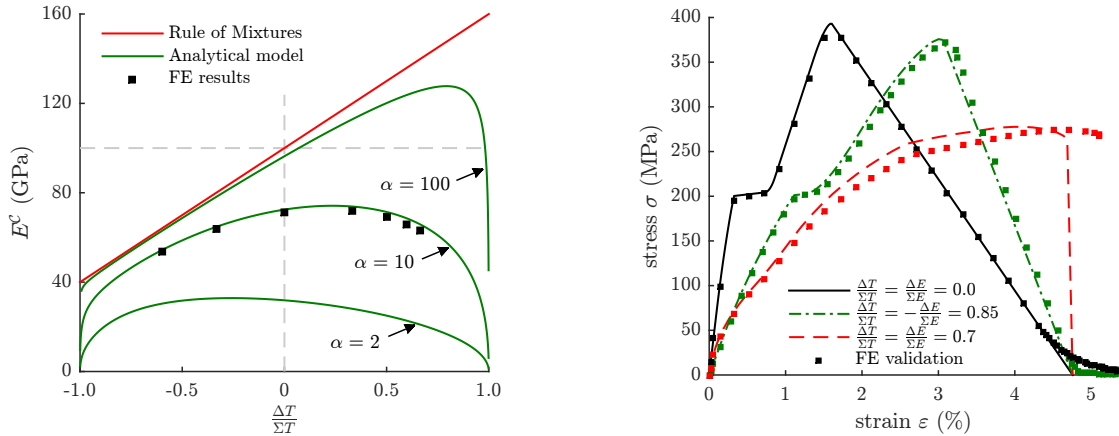
1. The model for hybrid “brick-and-mortar” composites (Section 2.1) is used to collect the stress-strain curve of each overlap of an *interface* between two neighbouring fibres (Fig. 2c). Considering the example of Fig. 2d before the formation of fibre breaks, the model is run for  $\delta l_{\text{overlap } 1}$  and  $\delta l_{\text{overlap } 2}$ . Results are then combined in series to find the stress-strain response of the interface;
2. Four interfaces are combined in parallel to calculate the stress-strain curve of a *fibre* (Figs. 2b and 2c). Each type of fibre has a stochastic strength following a Weibull distribution, hence the model identifies when and where failure will occur, and breaks are introduced in the fibres accordingly;
3. Once the geometry is updated, the behaviour of the interface is re-derived with new overlap lengths. For instance, in Fig. 2d, the load along the first overlap  $\delta l_1$  is carried by fibre  $\mathcal{A}$  only (as fibre  $\mathcal{B}$  is discontinuous on both sides of the overlap), and the “brick-and-mortar” model is run for  $\delta l_2$ ,  $\delta l_3$ ,  $\delta l_4$  and  $\delta l_5$ , which are then combined in series as in step 2 above;
4. Finally, the stress-strain curves of all fibres in the cross-section of a Representative Volume Element (RVE) are combined in parallel, and a combination in series of the cross-sections returns the overall material response (see Section 3.2 for results).

### 3. Results

#### 3.1. Hybrid “brick-and-mortar” composites

The model developed in Section 2.1 has been validated against Finite Element simulations, and results are shown in Fig. 3. The parameters used for this section are  $t_m = 0.01$  mm,  $\Sigma T = T^{\mathcal{A}} + T^{\mathcal{B}} = 0.2$  mm,

$\Sigma E = E^{\mathcal{A}} + E^{\mathcal{B}} = 200$  GPa and  $G^m = 1$  GPa. The effect of hybridisation has been studied by varying the difference of the thickness and stiffness of the two platelets, governed by the parameters  $\Delta E = E^{\mathcal{B}} - E^{\mathcal{A}}$  and  $\Delta T = T^{\mathcal{B}} - T^{\mathcal{A}}$ ; the effect of the aspect ratio of the platelets (defined as  $\alpha = 2 \cdot L/\Sigma T$ ) is also analysed.



(a) Effect of the difference in thickness of the two platelets ( $\Delta T$ ) on the stiffness of a composite, for  $\Delta E/\Sigma E = 0.6$  and different aspect ratios  $\alpha$ . (b) Full stress-strain curves for three different hybrid configurations, assuming a strain-hardening matrix.

**Figure 3.** Results and FE validation of the analytical model for hybrid “brick-and-mortar” composites.

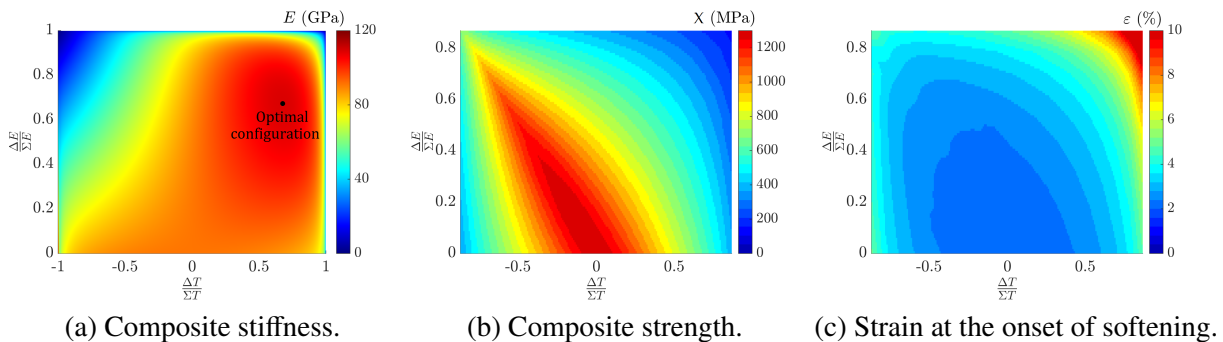


**Figure 4.** Parametric colourmaps for an aspect ratio  $\alpha = 50$ , assuming a bilinear matrix.

Fig. 3 shows good agreement between the analytical model and FE results. In particular, Fig. 3a shows that the conventional Rule of Mixtures (RoM) cannot be applied to predict the stiffness of hybrid “brick-and-mortar” materials, especially for low aspect ratios. Fig. 3b shows that varying the difference in thickness and stiffness of the platelets will affect the properties of the composite (ductility, stiffness and strength), therefore allowing the material to be tailored for specific applications.

Fig. 4 shows three colourmaps giving the evolution of the stiffness, strength, and onset of strain-softening of the composite with all possible hybrid configurations, for a fixed aspect ratio. These colourmaps, which are only feasible due to the fully analytical nature of the model, can be used to find optimal configurations and to support material development. Fig. 4a suggests that, for a given aspect ratio, maximizing the overall stiffness requires an optimal configuration with a certain amount of soft material (rather than simply minimising the soft material, as would be suggested by the RoM). Fig. 4b and 4c show opposite trends for the strength and onset of softening: while the strength increases when there is more of the soft platelets in the material, the strain at the onset of softening is larger for more of the stiff platelets (considering that failure of the composite is governed by failure of the matrix only).

### 3.2. Aligned intermingled hybrid composites

The model developed in Section 2.2 was compared against experiments on aligned hybrid intermingled composites, as shown in Fig. 5 and 6. The properties of the three types of fibres considered are given in Table 1; the volume fraction  $V_f = 35\%$  measured in the experiments was used for modelling.

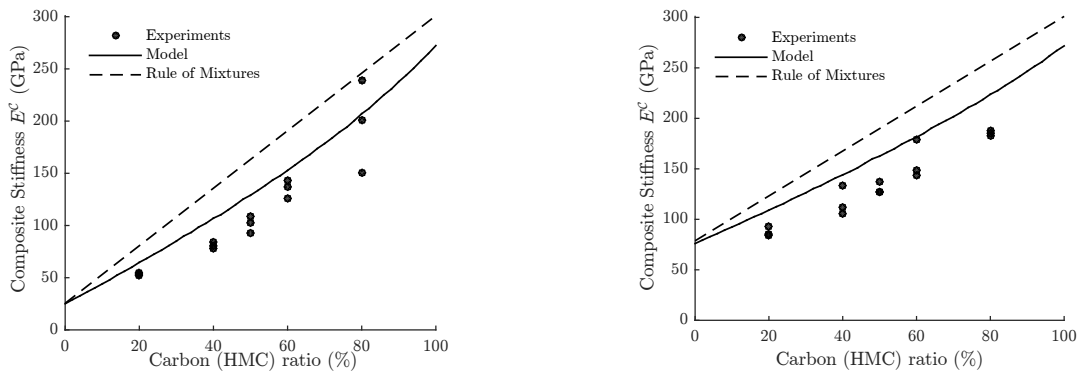
**Table 1.** Material properties of the fibres and matrix used in experiments, taken as inputs for the model (Fig. 5 and Fig. 6).

	$l_f$ (mm)*	$\phi$ ( $\mu\text{m}$ )*	$E$ (GPa)*	$m^\dagger$	$X$ (MPa)*	Matrix properties	
Glass	3.0	10	73	—	—	$G^m$ (GPa)	1.5
High Strength Carbon	3.0	7	225	5.71	4344	$S^m$ (MPa)	100
High Modulus Carbon	3.0	7	860	5.00	2230 $^\ddagger$	$\mathcal{G}_{llc}^m$ (kJ/m <sup>2</sup> )	2

\* From manufacturer [6].

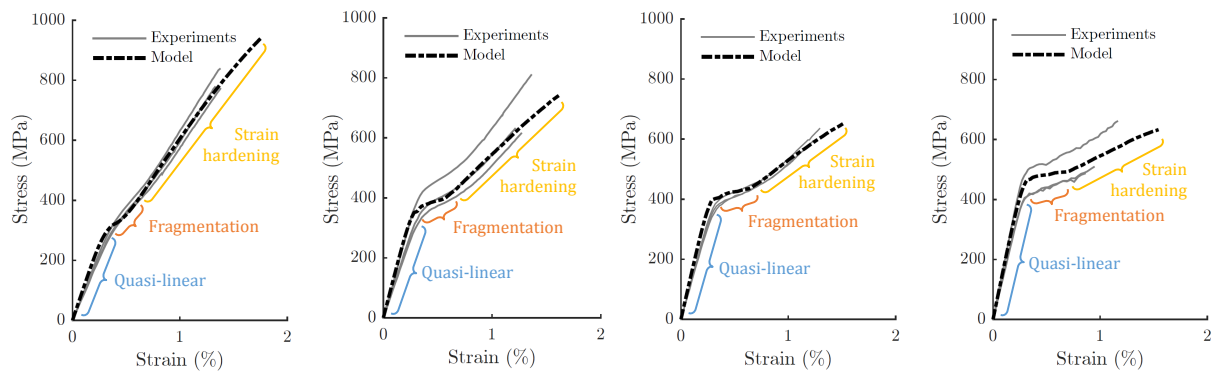
$^\dagger$  Derived from experimental results from literature [7, 8].

$^\ddagger$  Calibrated (with values from the manufacturer and literature [2, 6, 7]).



(a) High-Modulus Carbon / Glass hybrid. (b) High-Modulus Carbon / High-Strength Carbon hybrid.

**Figure 5.** Stiffness predictions from the proposed model and from the Rule of Mixtures compared against experiments, for different hybrid intermingled composites.



(a) 20%HMC-80%HSC. (b) 40%HMC-60%HSC. (c) 50%HMC-50%HSC. (d) 60%HMC-40%HSC.

**Figure 6.** Stress-strain curve predictions compared to experiments, considering different volume ratios of the two fibre types High-Modulus Carbon (HMC) and High-Strength Carbon (HSC).

Fig. 5 shows that the model has a better quantitative agreement with experiments than the RoM (as the former reflects the effect of the discontinuities and hybridisation), particularly for higher ratios of the stiffer fibres; the difference between the model and the experiment can be explained by fibre misalignments in the specimen. Moreover, the model can capture a non-linear trend in the stiffness of hybrid intermingled composites that the rule of mixture neglects.

Considering now the full stress-strain curves of intermingled hybrid composites, the behaviour of such composites can be separated in three main regions (Fig. 6):

1. *Quasi-linear* region: Both types of fibres carry the load, which leads to a quasi-linear response of the material (with any non-linearity being mostly due to damage of the matrix);
2. *Fragmentation* region: When the failure strain of the low-failure-strain fibres is reached, they start fragmenting and stop carrying load, leading to a decrease in the overall stiffness;
3. *Strain-hardening* region: Once the low-failure-strain phase is fully fragmented, the load is carried by the high-failure-strain fibres, until the final failure of the material.

Fig. 6 displays good agreement between the experiments and the model; the three regions defined above are found in both the model and the experiments. As more low-failure-strain fibres are added to the composite, the results suggest that (i) the fragmentation region becomes wider and more pronounced, and (ii) the strain-hardening region becomes less steep. These two effects will result in an increase of the overall strain to failure, therefore enhancing the material pseudo-ductility. The key achievements of this model are its ability to capture (i) the slope of the fragmentation region (which is often modelled by a plateau in former models) and (ii) a slight increase in the apparent failure-strain of the low-failure-strain fibres, known as the hybrid effect [9].

#### 4. Conclusion

A new model for hybrid "brick-and-mortar" composites was developed and validated against FE simulations. The model suggests that the rule of mixtures cannot be applied for short inclusions, as the composite response is governed mainly by the matrix behaviour for small aspect ratios. Moreover, the model showed — counter-intuitively — that, for short inclusions, the stiffness does not increase monotonically with the addition of stiffer material.

A new model for hybrid intermingled discontinuous composites has also been developed, and showed good agreement with experiments. In particular, this new model is able to capture non-linear responses in composites due to both breakage of the low-failure-strain fibres and non-linearity of the matrix.

These models can be used as tools to optimise hybrid configurations or to tailor materials for specific applications, and can therefore be adopted to support material development and perform virtual experiments.

#### Contributions and acknowledgements:

J. Henry and S. Pimenta developed the model and produced the modelling results presented in this paper. S. Pimenta acknowledges the support from the Royal Academy of Engineering in the scope of her Research Fellowship on *Multiscale discontinuous composites for large scale and sustainable structural applications* (2015-2019).

H. Yu and M. Longana manufactured and tested the intermingled hybrid specimens and provided the experimental data in Fig. 5 and 6. This work was funded under the EPSRC Programme Grant EP/I02946X/1 on High Performance Ductile Composite Technology. Supporting data can be requested from the corresponding author.

## References

- [1] Vikas Tomar, Tao Qu, Devendra K. Dubey, Devendra Verma, and Yang Zhang. *Multiscale Characterization of Biological Systems*. Springer-Verlag New York, 2015.
- [2] Hana Yu, Marco L Longana, Meisam Jalalvand, Michael R Wisnom, and Kevin D Potter. Pseudo-ductility in intermingled carbon / glass hybrid composites with highly aligned discontinuous fibres. *Composites Part A: Applied Science and Manufacturing*, 73:35–44, 2015.
- [3] François Barthelat and Reza Rabiei. Toughness amplification in natural composites. *Journal of the Mechanics and Physics of Solids*, 59(4):829–840, 2011.
- [4] Soraia Pimenta and Paul Robinson. An analytical shear-lag model for brick-and-mortar composites considering non-linear matrix response and failure. *Composites Science and Technology*, 104:111–124, 2014.
- [5] Meisam Jalalvand, Gergely Czél, and Michael R. Wisnom. Damage analysis of pseudo-ductile thin-ply UD hybrid composites - a new analytical method. *Composites Part A: Applied Science and Manufacturing*, 69:83–93, 2014.
- [6] Toho Tenax. The PAN based Carbon Fiber, DataSheet. page 18, 2010.
- [7] Kimiyoshi Naito, Yoshihisa Tanaka, Jenn-ming Yang, and Yutaka Kagawa. Tensile properties of ultrahigh strength PAN-based , ultrahigh modulus pitch-based and high ductility pitch-based carbon fibers. *Carbon*, 46:189–195, 2008.
- [8] Evaldo José Corat, Lays D. Ribeiro Cardoso, and Marinés C. Bravo Carvajal. Effect of the CVD parameters on the fiber tensile strength of carbon fibers using single-fiber tensile test after carbon nanotubes growth. In *INPE, São José dos Campos*, April 2015.
- [9] Yentl Swolfs, Ignaas Verpoest, and Larissa Gorbatikh. Maximising the hybrid effect in unidirectional hybrid composites. *Materials and Design*, 93:39–45, 2016.